Crystals **2011**, *1*, 244-253; doi:10.3390/cryst1040244

OPEN ACCESS

crystals

ISSN 2073-4352

www.mdpi.com/journal/crystals

Article

Defect *Scheelite*-Type Lanthanoid(III) *Ortho*-Oxomolybdates(VI) $Ln_{0.667}[MoO_4]$ (*Ln* = Ce, Pr, Nd, and Sm) and Their Relationship to *Zircon* and the NaTl-Type Structure

Tanja Schustereit, Sabine L. Müller, Thomas Schleid and Ingo Hartenbach *

Institute for Inorganic Chemistry, University of Stuttgart, Pfaffenwaldring 55, 70569 Stuttgart, Germany; E-Mails: schustereit@iac.uni-stuttgart.de (Ta.S.); mueller@iac.uni-stuttgart.de (S.L.M.); schleid@iac.uni-stuttgart.de (Th.S.)

* Author to whom correspondence should be addressed; E-Mail: hartenbach@iac.uni-stuttgart.de; Tel.: +49-711-685-64254; Fax: +49-711-685-54254.

Received: 14 October 2011; in revised form: 22 November 2011 / Accepted: 30 November 2011 / Published: 5 December 2011

Abstract The rare-earth metal(III) *ortho*-oxomolybdates with the formula $Ln_{0.667}[MoO_4]$ (*Ln* = Ce, Pr, Nd, and Sm) and defect *scheelite*-type structure crystallize in the tetragonal space group $I4_1/a$ (a = 533–525, c = 1183–1158 pm) with four formula units per unit cell. The Ln^{3+} cations at *Wyckoff* position 4*b* exhibit a coordination sphere of eight oxygen atoms in the shape of a trigonal dodecahedron. The same site symmetry ($\bar{4}$..) is observed for the tetrahedral oxomolybdate(VI) entities $[MoO_4]^{2-}$, since their central Mo^{6+} cation is situated at the 4*a* position. Due to this equal site multiplicity, the lanthanoid(III) cations have to be statistically under-occupied to maintain electroneutrality, thus a defect *scheelite* structure emerges. The partial structure of both the Ln^{3+} cations and the $[MoO_4]^{2-}$ anions (if shrunk to their centers of gravity) can be best described as distorted diamond-like arrangements. Therefore, these two interpenetrating partial structures exhibit a similar setup as found in the *zircon*-type as well as in the NaTl-type structure.

Keywords: lanthanoids; *ortho*-oxomolybdates; *scheelite*-type; crystal structure

1. Introduction

The mineral *scheelite* ($Ca[WO_4]$) is named after the German-Swedish pharmacist and chemist *Carl Wilhelm Scheele*, who, besides other elements, also discovered oxygen (independently from *Joseph Priestly*) and tungsten, and was able to synthesize tungstic acid from this mineral in the first place. The X-ray crystal structure of $Ca[WO_4]$ was originally published 1920 by *Dickinson* [1], but the positions of the oxygen atoms have not been determined. Besides *zircon* $Zr[SiO_4]$ [2], the *scheelite* structure is nature's favorite structure type for compounds containing larger cations (C.N. = 8 in case of both structure types) together with tetrahedral oxoanions. For trivalent rare-earth metal compounds, tetrahedral entities with pentavalent central atoms as counteranions, such as phosphates, arsenates and vanadates, are widely known. Besides compounds containing the larger lanthanide cations, which crystallize in the *monazite*-type (C.N.(Ln^{3+}) = 9) [3-8], rare-earth metal phosphates, arsenates and vanadates prefer the *xenotime*- ($Ln[PO_4]$) [4,7-11] and the *wakefieldite*-type $Ln[VO_4]$ [12,13], which are both equal to the *zircon*-type (C.N.(Ln^{3+}) = 8); only a high-pressure modification of $Sm[AsO_4]$ is known to crystallize in the *scheelite*-type [14]. Switching from tri- to $[MoO_4]^{2-}$ dianions, the trivalent lanthanide cations have to be either mixed with monovalent, mostly alkali metal, cations (*e.g.* $NaLa[MoO_4]_2$ [15]) or a deficiency on the atomic site prevails, which is known to the literature so far only for $Nd_{0.667}[MoO_4]$ [16]. In this paper, we focus on the close relationship between the *scheelite*-type ($Ca[WO_4]$, here: the title compounds $Ln_{0.667}[MoO_4]$, *Ln* = Ce, Pr, Nd, and Sm) and the *zircon*-type structure ($Zr[SiO_4]$), which can both be derived from the crystal structure of sodium thallide (NaTl) [17].

2. Results and Discussion

2.1. Structure Description of Scheelite-*Type* $Ln_{0.667}[MoO_4]$

The rare-earth metal(III) *ortho*-oxomolybdates(VI) of the empirical formula $Ln_{0.667}[MoO_4]$ (*Ln* = Ce, Pr, Nd, and Sm) in the defect *scheelite*-type structure crystallize tetragonally with the space group $I4_1/a$ (a = 533–525, c = 1183–1158 pm) and four formula units per unit cell. In their crystal structure one crystallographically unique lanthanoid trication is present at *Wyckoff* position 4*b* (see Table 1 site symmetry: $\bar{4}$..), showing a coordination sphere of eight oxygen atoms in the shape of a trigonal dodecahedron (Figure 1, *left top*). The distances between the Ln^{3+} cations and their surrounding O^{2-} anions range between 255 pm for the cerium compound, the largest of the four lanthanoid representatives, and 249 pm in the samarium derivative, the smallest one in this case (see Table 2). These distances are in good agreement with those of other rare-earth metal compounds with complex oxoanions such as the *monazite*-type phosphates with the formula $Ln[PO_4]$ ($Ce[PO_4]$: $d(Ce^{3+}–O^{2-})$ = 245–265 pm; $Sm[PO_4]$: $d(Sm^{3+}–O^{2-})$ = 239–259 pm) [4]. To maintain electroneutrality, the atom site of the Ln^{3+} cations cannot be fully occupied, but by about two thirds, which is the case for all four title compounds (see Table 1). The molybdenum(VI) cations are also crystallographically unique and situated at the *Wyckoff* position 4*b* (see Table 1, site symmetry: $\bar{4}$..). They are surrounded by four oxygen atoms forming bisphenoidally distorted tetrahedra whose molybdenum–oxygen bond lengths, as well as their O–Mo–O angles, do not vary much throughout the presented series ($d(Mo^{6+}–O^{2-})$ = 175–177 pm, $\sphericalangle(O^{2-}–Mo^{6+}–O^{2-})$ = 107–108°, 4×, and 114–116°, 2×, see Table 2). For

comparison, the Mo–O bond lengths and angles found in *powellite* (*scheelite*-type Ca[MoO_4]) lie at 176 pm, 107° (4×), and 115° (2×) [18] and thus agree very well with the herein presented data for the title compounds. The isolated $[MoO_4]^{2-}$ tetrahedra (see Figure 1, *left bottom*) are exclusively vertex-connected to the polyhedra around the Ln^{3+} cations, therefore the crystallographically unique O^{2-} anions are surrounded by one molydenum and two lanthanoid cations. The crystal structure of the $Ln_{0.667}[MoO_4]$ series (*Ln* = Ce, Pr, Nd, and Sm) is shown in Figure 1, on the right.

Table 1. Fractional atomic coordinates, site occupation probabilities, and coefficients of the equivalent isotropic displacement parameters (U_{eq} [a]/pm^2) in the crystal structures of the *scheelite*-type series $Ln_{0.667}[MoO_4]$ (*Ln* = Ce, Pr, Nd, and Sm).

***Ln* = Ce**	***Wyckoff* position**	***x*/*a***	***y*/*b***	***z*/*c***	***s. o. f.*** [b]	**occupation percentage**	U_{eq} [a]
Ce	4*b*	0	¼	⅝	0.1678(3)	67.12(3) %	121(2)
Mo	4*a*	0	¼	⅛	0.25	100 %	139(2)
O	16*f*	0.1406(3)	0.0112(3)	0.2067(2)	1.0	100 %	288(5)
***Ln* = Pr**							
Pr	4*b*	0	¼	⅝	0.1654(6)	66.16(6) %	80(3)
Mo	4*a*	0	¼	⅛	0.25	100 %	124(3)
O	16*f*	0.1406(6)	0.0096(7)	0.2062(3)	1.0	100 %	299(10)
***Ln* = Nd**							
Nd	4*b*	0	¼	⅝	0.1685(7)	67.40(7) %	107(3)
Mo	4*a*	0	¼	⅛	0.25	100 %	132(4)
O	16*f*	0.1458(9)	0.0099(9)	0.2049(4)	1.0	100 %	256(10)
***Ln* = Sm**							
Sm	4*b*	0	¼	⅝	0.1632(4)	65.28(4) %	102(3)
Mo	4*a*	0	¼	⅛	0.25	100 %	128(3)
O	16*f*	0.1477(4)	0.0097(4)	0.2078(2)	1.0	100 %	254(6)

[a] U_{eq} is defined as the ⅓ of the trace of the orthogonalized U_{ij} tensor [19]; [b] s. o. f. = site occupation factor.

Table 2. Selected interatomic distances and bond angles in the crystal structures of the *scheelite*-type series $Ln_{0.667}[MoO_4]$ (*Ln* = Ce, Pr, Nd, and Sm).

$Ce_{0.667}[MoO_4]$			
d(Ce^{3+}–O^{2-})	4 × 254.3(2) pm	d(Mo^{6+}–O^{2-})	4 × 176.6(2) pm
	4 × 255.8(2) pm	∢(O^{2-}–Mo^{6+}–O^{2-})	4 × 107.5(1)°
d(Ce^{3+}···Mo^{6+})	4 × 376.9(2) pm		2 × 113.6(1)°
	4 × 398.2(2) pm		
$Pr_{0.667}[MoO_4]$			
d(Pr^{3+}–O^{2-})	4 × 253.5(4) pm	d(Mo^{6+}–O^{2-})	4 × 176.5(3) pm
	4 × 254.7(3) pm	∢(O^{2-}–Mo^{6+}–O^{2-})	4 × 107.1(1)°
d(Pr^{3+}···Mo^{6+})	4 × 376.4(3) pm		2 × 114.3(2)°
	4 × 397.0(3) pm		
$Nd_{0.667}[MoO_4]$			
d(Nd^{3+}–O^{2-})	4 × 250.0(4) pm	d(Mo^{6+}–O^{2-})	4 × 175.2(5) pm
	4 × 253.6(5) pm	∢(O^{2-}–Mo^{6+}–O^{2-})	4 × 106.5(2)°
d(Nd^{3+}···Mo^{6+})	4 × 373.3(4) pm		2 × 115.6(3)°
	4 × 393.8(4) pm		

Table 2. *Cont.*

$Sm_{0.667}[MoO_4]$			
d(Sm^{3+}–O^{2-})	4 × 249.0(2) pm 4 × 249.3(2) pm	d(Mo^{6+}–O^{2-}) ∢(O^{2-}–Mo^{6+}–O^{2-})	4 × 176.4(2) pm 4 × 107.2(1)° 2 × 114.2(1)°
d(Sm^{3+}···Mo^{6+})	4 × 371.3(2) pm 4 × 390.9(2) pm		

Figure 1. Anionic environment around the crystallographically unique Ln^{3+} cations (*left top*, thermal ellipsoids at 90% probability), cationic environment around the crystallographically unique $[MoO_4]^{2-}$ tetrahedra (*left bottom*, thermal ellipsoids at 90% probability), and view at the unit cell of the defect *scheelite*-type crystal structure of the $Ln_{0.667}[MoO_4]$ series (*Ln* = Ce, Pr, Nd, and Sm) along [010] (*right*).

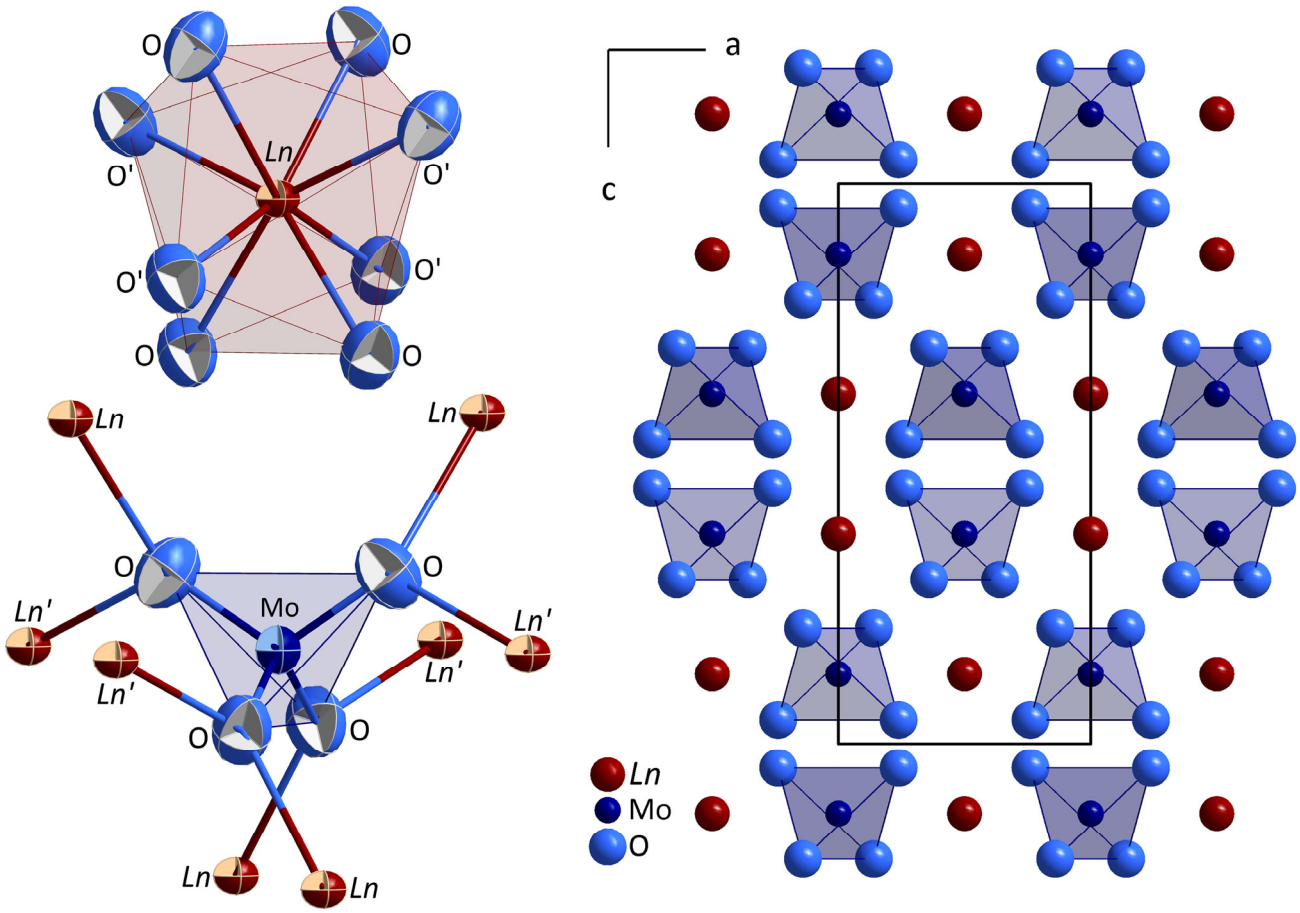

2.2. The Structural Relationship Between the Scheelite-*Type, the* Zircon-*Type, and the NaTl-Type Structure*

A simple structure type for compounds containing complex building blocks can usually be determined when the complex unit is shrunk to its center of gravity. In the case of the *scheelite*-type structure, the result can be considered as an *AB* structure with a coordination number ratio of 8:8. The first structure type that comes to mind with these "real" coordination numbers would be cesium chloride (CsCl) [20], but no further similarity can be found between these two structures. Interconnecting the Ln^{3+} and the Mo^{6+} cations with themselves, they show a tetrahedral coordination

environment towards each other and; thus, the structure ends up in two interpenetrating *diamond*-like lattices [21] (Figure 2, *middle*), which is the description of the NaTl-type structure [17] (Figure 2, *left*). The same is also true considering *zircon*-type structures [2] if stripped off the ligand O^{2-} anions (Figure 2, *right*).

Figure 2. Excerpt from the crystal structures of NaTl (*left*), *scheelite* $Ca[WO_4]$ (*middle*, here: $Ln_{0.667}[MoO_4]$), and *zircon* $Zr[SiO_4]$ (*right*) with special emphasis on the interpenetrating *diamond*-like lattices resulting from the "deoxygenated" structures.

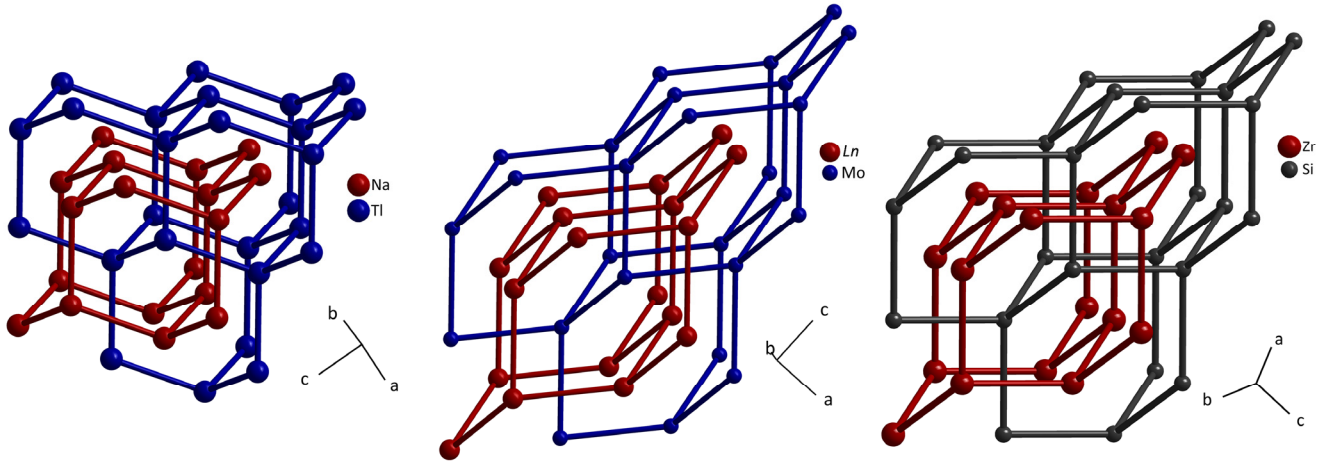

In the crystal structure of sodium thallide each Tl^- anion is surrounded by ten Na^+ cations and four Tl^- anions resulting in an overall coordination number of 14. If only the sodium cations are considered, the thallium atoms are enclosed by *adamantane*-like cage with four shorter (323 pm, Na in Figure 3, *left*) and six longer distances (373 pm, Na' in Figure 3, *left*). While the longer-bonded $(Na')^+$ cations form an octahedron around the central Tl^- anion, the shorter connected $(Na)^+$ cations arrange themselves tetrahedrally, building up a heterocuban cage together with the four next thallium neighbors, which show the same distance to the center as the four closest Na^+ cations. *Vice versa*, the same is of course true, if the environment of Na^+ is described. This symmetrically ideal setup (NaTl: cubic, F*d*$\bar{3}$*m*, *a* = 748.8(3) pm [17], Na at Wyckoff position 8*a*, Tl in 8*b*, both with site symmetry $\bar{4}$3m) is tetragonally distorted in the *scheelite*-type structure (site symmetry: $\bar{4}$.. for both Ln^{3+} and Mo^{6+}). Therefore eight short (≈ 375 pm, 4× and ≈ 400 pm, 4×) and two long distances (≈ 590 pm, 2×) between Mo^{6+} and Ln^{3+} are determined in the alike *adamantane* cage of Ln^{3+} around the Mo^{6+} (and thus around the $[MoO_4]^{2-}$ anions) with the four closest neighbors (*Ln* in Figure 3, *middle*) forming a square plane around the central Mo^{6+} cation and the four slightly more distant ones (*Ln'* in Figure 3, *middle*) arrange tetrahedrally like the $(Na)^+$ cations in NaTl. Here also the description of the Ln^{3+} environment around the oxomolybdate unit can be interchanged to the alternative situation. In the case of the the *zircon*-type structure ($Zr[SiO_4]$: tetragonal, *I*4$_1$/*amd*, *a* = 660.7(1), *c* = 598.2(1) pm [22], Zr at the *Wyckoff* position 4*a*, Si at 4*b*, both with site symmetry $\bar{4}$*m*2) a further distortion of the aforementioned arrangement is detectable. Again, four out of the ten Zr^{4+} cations of the *adamantane* cage build a tetrahedron around the central Si^{4+} cation (and thus around the $[SiO_4]^{4-}$ anion). However, in this structure type once again these four are not the nearest surrounding atoms (363 pm, Zr' in Figure 3, *right*), but two of the remaining six show a very short $Zr^{4+}\cdots Si^{4+}$ distance of 299 pm (Zr in Figure 3, *right*). The other four are about 170 pm further away (467 pm, Zr'' in Figure 3,

right). This distortion is easily explained by the interconnection of the tetrahedral complex oxoanion with the anionic polyhedra around the Zr^{4+} cations. While in the *scheelite* structure these are exclusively vertex-connected (at all eight O^{2-} anions), in the *zircon* structure two edges and four vertices are the joining links, and the aforementioned short zirconium–silicon distances of 299 pm are those running through the connecting edges. Here again the partial structures around Zr^{4+} and $[SiO_4]^{4-}$ can be interchanged.

Figure 3. *Adamantane*-like cages of Na^+ around Tl^- in NaTl (*left*), of Ln^{3+} around $[MoO_4]^{2-}$ in the *scheelite* structure (*middle*), and of Zr^{4+} around $[SiO_4]^{4-}$ in the *zircon* structure (*right*).

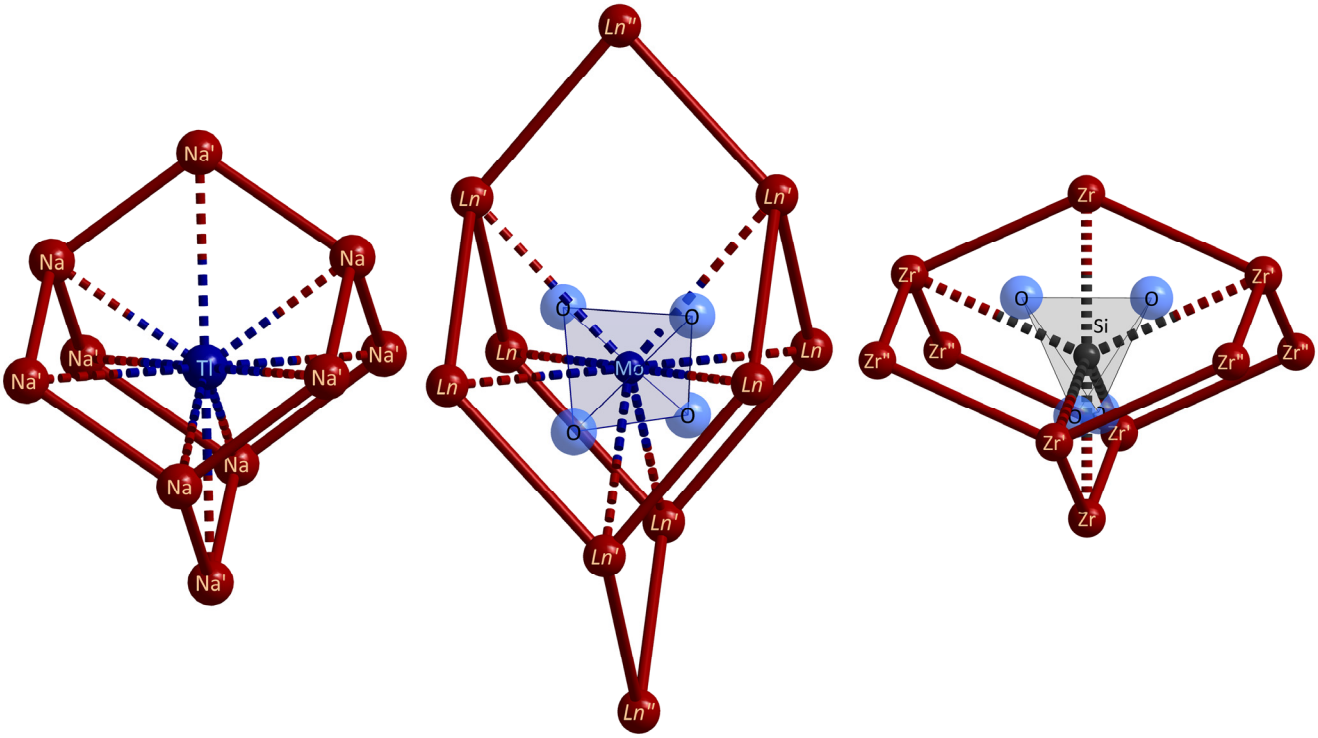

In general, the *adamantane* cage can be dismembered resulting in an octahedron with an interpenetrating tetrahedron. While the tetrahedron contributes to the linking in all three cases (Figure 3: Na in NaTl, *Ln'* in *scheelite*-type $Ln_{0.667}[MoO_4]$, and Zr' in *zircon*-type $Zr[SiO_4]$), in the case of the octahedron, only for NaTl do all six members show the same distance to the central Tl^- anion. For *scheelite*-type compounds the octahedron is stretched, leaving two very far (*Ln*'') and four short (*Ln*) contacts behind, and in *zircon*-type compounds it is compressed, comprising two very short (Zr) and four long (Zr'') distances to the central unit. In all cases the structures can also be described *vice versa*.

3. Experimental Section

3.1. Synthesis

All four representatives of the short $Ln_{0.667}[MoO_4]$ series (Ln = Ce, Pr, Nd, and Sm) were only obtained as by-products so far. The direct synthesis using Ln_2O_3 and MoO_3 in 1:3 molar ratios experiences a direct competition with the rare-earth metal "sesquimolybdates" $Ln_2[MoO_4]_3$ (better: $Ln_2Mo_3O_{12}$ since not all of the these structures contain isolated $[MoO_4]^{2-}$ units), which are known in literature for some of the rare-earth elements, comprising *Ln* = Ce [23], Nd [16], and Sm [24], although in different structure types, depending on the size of the lanthanoid. In the case of $Ce_{0.667}[MoO_4]$, the single crystals emerged from an unsuccessful attempt to synthesize $Ce[MoO_4]_2$. $Pr_{0.667}[MoO_4]$ and $Sm_{0.667}[MoO_4]$ were obtained in experiments planned to prepare the respective fluoride oxodimolybdates $PrFMo_2O_7$ and $SmFMo_2O_7$ [25], and the neodymium representative $Nd_{0.667}[MoO_4]$ occurred as by-product in the synthesis of $NdBr[MoO_4]$ [26]. The single crystals of all four title compounds are coarse, transparent and remain stable when exposed to air and water. They show the color of the respective Ln^{3+} cation, *i. e.* green in the case of Pr, violet for Nd, and pale yellow for Sm. The crystals of the cerium derivative display an orange color, which is not quite uncommon, since very often in cerium(III) compounds the transition energy is lowered and the compound exhibits a color in the range between yellow and red, depending on the actual chemical surrounding of the Ce^{3+} cations. This can be assigned to the effect that the orbital, which contains the single f-electron lies within the band gap between the valence and the conduction band [27,28].

3.2. X-ray Structure Analysis

Intensity data sets for single crystals of all four $Ln_{0.667}[MoO_4]$ representatives (*Ln* = Ce, Pr, Nd, and Sm) were collected on a Nonius Kappa-CCD diffractometer using graphite-monochromatized Mo-Kα radiation (wavelength: λ = 71.07 pm). A numerical absorption correction was performed with the help of the program HABITUS [29]. The structure solutions and refinements were carried out by using the program package SHELX-97 [30]. Details of the data collections and the structure refinements [31] are summarized in Table 3, atomic positions and coefficients of the equivalent isotropic displacement parameters [19] can be found in Table 1, while interatomic distances and selected bond angles are listed in Table 2. Further details of the crystal structure investigations can be obtained from the Fach-informationszentrum (FIZ) Karlsruhe, D-76344 Eggenstein-Leopoldshafen, Germany (Fax: +497247-808-666; E-Mail: crysdata@fiz-karlsruhe.de), on quoting the depository numbers CSD-423509 for $Ce_{0.667}[MoO_4]$, CSD-423510 for $Pr_{0.667}[MoO_4]$, CSD-423511 for $Nd_{0.667}[MoO_4]$, and CSD-423512 for $Sm_{0.667}[MoO_4]$.

Table 3. Crystallographic data for *scheelite*-type series $Ln_{0.667}[MoO_4]$ (*Ln* = Ce, Pr, Nd, and Sm), tetragonal crystal system, space group: $I4_1/a$, $Z = 4$, corrections for background, polarization and Lorentz factors applied as well as a numerical absorption correction with the program HABITUS [29], scattering factors according to International Tables, Vol. C [31].

Ln	**Ce**	**Pr**	**Nd**	**Sm**
Lattice constants, a/pm	533.07(3)	532.27(3)	527.94(3)	525.09(3)
c/pm	1183.33(7)	1178.56(7)	1169.12(7)	1158.38(7)
c/a	2.220	2.214	2.214	2.206
Calculated density, D_x/g·cm^{-3}	5.005	5.051	5.220	5.411
Molar volume, V_m/cm^3·mol^{-1}	50.63	50.27	49.06	48.08
F(000)	450.7	453.4	456.0	461.4
Index range, $\pm h/\pm k/\pm l$	7/7/15	7/7/15	6/7/14	6/6/15
Theta range, $\theta_{min} - \theta_{max}$/deg	4.2 – 28.3	4.2 – 28.2	4.2 – 28.3	4.3 – 28.1
Absorption coefficient, μ/mm^{-1}	12.53	13.25	14.25	15.94
Collected/unique reflections/parameters	2298/209/16	2290/206/16	1444/202/16	2492/196/16
R_{int}/R_σ	0.039/0.016	0.082/0.030	0.073/0.042	0.063/0.020
R_1 for (n) refletions with $\lvert F_o\rvert \geq 4\sigma(F_o)$	0.014 (n = 173)	0.020 (n = 121)	0.019 (n = 96)	0.016 (n = 164)
R_1/wR_2 for all reflections	0.018/0.030	0.045/0.040	0.068/0.040	0.021/0.036
Goodness of Fit (GooF)	1.082	1.038	0.925	1.107
Extinction, g	0.0103(6)	0.0040(6)	0.0033(4)	0.0123(8)
Residual electron density, ρ/e$^-$·10^{-6} pm^{-3}, min./max.	0.34/–0.35	0.51/–0.43	0.46/–0.57	0.33/–0.41

4. Conclusions

Single crystals of four representatives of lanthanoid(III) oxomolybdates(VI) with deficient *scheelite*-type structure according to $Ln_{0.667}[MoO_4]$ (*Ln* = Ce, Pr, Nd, and Sm) were obtained from the corresponding oxides (Ln_2O_3 and MoO_3) as by-products in various synthetic experiments. Their crystal structure was determined and described in detail. Furthermore, the structural setup of the *scheelite*-type ($Ca[WO_4]$) was compared to that of the *zircon*-type ($Zr[SiO_4]$), which are both distortion varieties of the NaTl-type structure with two interpenetrating diamond-like sublattices.

Acknowledgments

The financial support of the *German Research Foundation* (DFG, Bonn, Germany) and the *State of Baden-Württemberg* (Stuttgart, Germany) is gratefully acknowledged.

References and Notes

1. Dickinson, R.G. The Crystal Structure of Wulfenite and Scheelite. *J. Am. Chem. Soc.* **1920**, *42*, 85-93.
2. Hassel, O. Die Kristallstruktur einiger Verbindungen von der Zusammensetzung MRO_4. I. Zirkon $ZrSiO_4$. *Z. Kristallogr.* **1926**, *63*, 247-254.
3. Mooney, R.C.L. Crystal Structures of a Series of Rare Earth Phosphates. *J. Chem. Phys.* **1948**, *16*, 1003-1003.
4. Ni, Y.-X.; Hughes, J.M.; Mariano, A.N. Crystal Chemistry of the Monazite and Xenotime Structures. *Amer. Miner.* **1995**, *80*, 21-26.
5. Brusset, H.; Madaule-Aubry, F.; Mahe, R.; Boursier, C. Chimie Structurale - Étude de la Structure de l'Orthovanadate de Lanthane. *C. R. Hebd. Seances Acad. Sci.* **1971**, *273*, 455-458.
6. Brahimi, A.; Ftini, M.M.; Amor, H. Cerium Arsenate, $CeAsO_4$. *Acta Crystallogr.* **2002**, *E58*, 98-99.
7. Schmidt, M.; Müller, U.; Cardoso-Gil, R.; Milke, E.; Binnewies, M. Zum chemischen Transport und zur Kristallstruktur von Seltenerdarsenaten(V). *Z. Anorg. Allg. Chem.* **2005**, *631*, 1154-1162.
8. Kang, D.-H.; Schleid, Th. Einkristalle von La[AsO_4] im Monazit- und Sm[AsO_4] im Xenotim-Typ. *Z. Anorg. Allg. Chem.* **2005**, *631*, 1799-1802.
9. Vegard, L. Structure of Xenotime and Relations Between Chemical Constitution and Crystal Structure. *Philos. Mag.* **1927**, *4*, 511-525.
10. Schäfer, W.; Will, G. Neutron Diffraction Study of Antiferromagnetic $DyAsO_4$. *J. Phys.* **1971**, *C 4*, 3224-3233.
11. Kang, D.-H.; Höss, P.; Schleid, Th. Xenotime-Type Yb[AsO_4]. *Acta Crystallogr.* **2005**, *E61*, i270-i272.
12. Broch, E. Die Kristallstruktur von Yttriumvanadat. *Z. Phys. Chem. B* **1933**, *20*, 345-350.
13. Milligan, W.O.; Vernon, L.W. Crystal Structure of Heavy Metal Orthovanadates. *J. Phys. Chem.* **1952**, *56*, 145-148.
14. Kang, D.-H.; Schleid, Th. Einkristalle von Sm[AsO_4] im *Scheelit*-Typ. *Z. Anorg. Allg. Chem.* **2006**, *632*, 2147-2147.
15. Stevens, S.B.; Morrison, C.A.; Allik, T.H.; Rheingold, A.L.; Haggerty, B.S. $NaLa(MoO_4)_2$ as a Laser Host Material. *Phys. Rev. B: Condens. Matter.* **1991**, *43*, 7386-1394.
16. Jamieson, P.B.; Abrahams, S.C.; Bernstein, J.L. Crystal Structure of the Transition-Metal Molybdates and Tungstates. V. Paramagnetic α-$Nd_2[MoO_4]_3$. *J. Chem. Phys.* **1969**, *50*, 86-94.
17. Zintl, E.; Dullenkopf, W. Über den Gitterbau von NaTl und seine Beziehung zu den Strukturen vom Typus des β-Messings. *Z. Phys. Chem. B* **1932**, *16*, 195-205.
18. Aleksandrov, V.B.; Gorbatyii, L.V.; Ilyukhin, V.V. Crystal Structure of Powellite Ca[MoO_4]. *Kristallografiya* **1968**, *13*, 512-513.
19. Fischer, R.X.; Tillmanns, E. The Equivalent Isotropic Displacement Factor. *Acta Crystallogr.* **1988**, *C44*, 775-776.
20. Davey, W.P.; Wick, F.G. Crystal Structures of CsCl and TlCl. *Phys. Rev.* **1921**, *17*, 403-404.
21. Hull, W.H.; Bragg, W.L. Structure of some Crystals. *Proc. R. Soc. London Ser. A* **1913**, *33*, 277-277.

22. Robinson, K.; Gibbs, K.V.; Ribbe, P.H. The Structure of Zircon: A Comparison with Garnet. *Am. Mineral.* **1971**, *56*, 782-789.
23. Hartenbach, I. Crystal Structure of $Ce_2Mo_3O_{12}$, University of Stuttgart, Germany. Unpublished Results, 2010.
24. Hartenbach, I. Die Kristallstruktur von Samarium-Sesquimolybdat $Sm_2[MoO_4]_3$. *Z. Anorg. Allg. Chem.* **2008**, *634*, 2044-2044.
25. Müller, S.L. Synthese und Charakterisierung von Selten-Erd-Metall Fluorid Dimolybdaten. Exam Thesis, University of Stuttgart, 2012. In Preparation.
26. Schustereit, T. Die Reihe der Seltenerdmetall(III)-Bromid-Oxomolybdate(VI) und die Kristallstrukturen zweier Nebenprodukte. Exam Thesis, University of Stuttgart, 2010.
27. Dieke, G.H. *Spectra and Energy Levels of Rare Earth Ions in Crystals*; Interscience Publishers: New York, NY, USA, 1969.
28. Dorenbos, P. Absolute Location of Lanthanide Energy Levels and the Performance of Phosphors. *J. Lumin.* **2007**, *122-123*, 315-317.
29. Herrendorf, W.; Bärnighausen, H. *HABITUS: Program for the Optimization of the Crystal Shape for Numerical Absorption Correction in X-SHAPE*, version 1.06; Fa. Stoe: Darmstadt/Karlsruhe/Gießen, Germany, 1999/1993/1996.
30. Sheldrick, G.M. A short history of SHELX. *Acta Crystallogr.* **2008**, *A64*, 112-122.
31. Hahn, T.; Wilson, A.J.C. *International Tables for Crystallography*, 2nd ed.; Kluwer Academic Publishers: Boston, MA, USA, 1992; Volume C.